Parallel NMR Based on Solution Magnetic-Susceptibility Differences. Application to Isotopic Effects on Self-Diffusion†

Pascal H. Fries* and Daniel Imbert

CEA, INAC, Service de Chimie Inorganique et Biologique (UMR-E 3 CEA UJF, FRE 3200 CNRS), 38054 Grenoble, France

Different susceptibility NMR line shifts can be induced in distinct liquid solutions by dissolving different concentrations of complexes of paramagnetic lanthanide Ln^{3+} ions. We show how these solutions, put in capillaries, can be simultaneously studied with a standard high-resolution spectrometer. After theoretical justification the method is illustrated by an investigation of the effects of H/D substitution on self-diffusion in heavy water. Non-Stokesian effects are observed.

Introduction

The transport or move of molecules from one place to another, which is very common in physical and chemical processes, has attracted much attention in the domain of electrolyte solutions.[1] Under the action of external forces, macroscopic numbers of particles flow with velocities proportional to these forces. The proportionality factors, named mobilities, are themselves proportional to the diffusion coefficients of the particles according to the Einstein relation. Practical and reliable methods for predicting the general transport phenomena, which are so important in applied research, are still lacking despite notable theoretical advances since the beginning of the 1990s.[1,2] An ubiquitous kind of transport at the molecular scale is self-diffusion, that is, the random translational motion of a particle due to its bombardment by the neighboring molecules. Self-diffusion is one of the simplest properties, the macroscopic study of which allows one to test molecular theories of time-dependent phenomena in liquids.[3,4] It is one of the key molecular factors which govern the intermolecular NMR relaxation rates, and the determination of which is necessary to properly interpret these rates in terms of molecular interactions.[5–8] A fundamental result is the Stokes−Einstein eq 1 giving the self-diffusion coefficient D of a spherical particle of radius a in a liquid of viscosity η.

$$D = k_B T/(6\pi a\eta) \quad (1)$$

This equation was initially derived for a diffusing macroscopic solute which undergoes the frictional force of the neighboring solvent molecules approximated as a viscous continuum. However, it turns out to be surprisingly accurate even for a molecular solute, if the viscosity is replaced by an effective viscosity $f_t\eta$ where f_t is a translational (t) microviscosity factor depending only on the solute and solvent sizes.[9–11] Perhaps, one of the most remarkable features of the Stokes−Einstein expression is that D is independent of the solute and solvent masses, though it is a dynamical property which determines the mean squared displacement $\langle||\mathbf{R}(t)||^2\rangle = 6Dt$ of the solute as a function of time. Isotopic substitution is a natural method for studying the effect of the change of molecular mass on diffusion.[12] Accurate measurements are needed to quantify this small effect and interpret it in terms of theoretical models. The method should be convenient because the accompanying change of intermolecular potentials, which may affect D, is expected to be rather modest. The applicability of the Stokes−Einstein equation to molecular solutes can be questioned, first in the simplest case of pure liquids for which the solute and solvent molecules are the same species. For that purpose, an accurate NMR spin−echo procedure was developed by Holz et al.[13–15] For several liquids, they found a strong correlation between D and the inverse of the square roots of the moments of inertia of the molecule, indicating a translation−rotation coupling, but for a few liquids they observed that D varies as the inverse of the square root of the molecular mass as already predicted in dilute gases.[16] They concluded that the dependence of the diffusion coefficients on the molecular mass was still an open question, even in pure liquids. Liquid mixtures and solutions are the second class of liquids concerned by the Stokes−Einstein equation,[17,18] in particular those in which the solvent and diffusing solute have significantly different molecular masses. For instance, Weingärtner did not detect any isotopic effect on the self-diffusion of water, methanol, and ethanol amid the much heavier carbon tetrachloride molecules.[17] Clearly, more numerous experimental data are required to obtain a reliable overview of the dynamic isotopic effect in liquids.[15,19]

We present a high-resolution NMR parallel method for fast comparison of self-diffusion coefficients. The self-diffusion coefficients of the molecules carrying the observable nuclear spins are derived from pulsed (field-) gradient spin−echo (PGSE) experiments,[20,21] that is, from the attenuation of the spin−echo NMR signal caused by the molecular Brownian displacements. Parallelism is obtained by labeling the spins with resonance frequency shifts due to prescribed paramagnetic changes of the magnetic volume susceptibility of the solution. Such changes result from the controlled dissolution of paramagnetic solutes. They are at the basis of the Evans method for determining the paramagnetic susceptibility of such solutes, which simply requires a standard NMR tube containing one capillary tube in a preferred coaxial position.[22–25] Variants of the Evans method have been used to study properties of paramagnetic lanthanide Ln^{3+} complexes such as the crystal field of their ligands or their concentration.[26,27] Starting from the theory of the demagnetizing field, already revisited to investigate the effects of the geometry of the NMR sample on the line shape,[28] we show that parallel capillaries inside a standard NMR

† Part of the "Josef M. G. Barthel Festschrift".

* Corresponding author. Tel.: +33438783107; fax: +33438785090; e-mail: pascal-h.fries@cea.fr.

10.1021/je901031b © 2010 American Chemical Society
Published on Web 03/23/2010

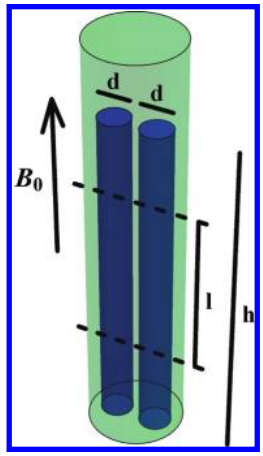

Figure 1. Capillary setup in a standard NMR tube.

tube can become independent tracks where the race of the diffusing molecules can occur. We explain why tiny variable concentrations of paramagnetic lanthanide Ln^{3+} complexes are particularly appropriate to yield the desired shifts. We apply the method to methanol, *tert*-butanol (tBuOD), and tetraphenylphosphonium (TPP) ions and some of their deuterated derivatives in D_2O.

Demagnetizing Field and Capillary Setup

We wish to simultaneously investigate the self-diffusion coefficients of n molecules M_i $(1 \le i \le n)$ in n different solutions sol_i of volume susceptibilities χ_i. The different susceptibilities obtained by varying the nature and/or concentrations of the paramagnetic solutes can be written as

$$\chi_i = \chi_{\text{dia}} + \chi_{\text{para},i} \tag{2}$$

where χ_{dia} and $\chi_{\text{para},i}$ are the susceptibilities of the solvent and solutes, respectively. To simplify the formulas and discussion, we assume that the molecules M_i are derived from one another by hydrogen/deuterium (H/D) isotopic substitution and that the observed proton spins I on M_i have the same chemical shift in all of the solutions. The formulas can be easily generalized to account for chemical shift variations. The experimental setup is sketched in Figure 1.

The solutions sol_i are put in identical glass or quartz capillaries where they occupy cylindrical columns C_i of equal heights h and diameters d. The capillaries are placed at the same height in a standard NMR tube located in the uniform vertical magnetic field $\mathbf{B}_0 = B_0\mathbf{k}$ of the cryomagnet of a high-resolution spectrometer. The liquid columns are centered with respect to the detection zone of the receiver coil, so that their upper and lower surfaces $S_{\text{up},i}$ and $S_{\text{low},i}$ are at quite large distances from the limits of the detection zone of length l. Consider a proton I at the position $\mathbf{r}_I$ in the capillary C_i. The local magnetic field $\mathbf{B}(\mathbf{r}_I)$ at $\mathbf{r}_I$ is $\mathbf{B}(\mathbf{r}_I) = \mathbf{B}_0 + \mathbf{B}_{\text{dip}}(\mathbf{r}_I)$, where $\mathbf{B}_{\text{dip}}(\mathbf{r}_I)$ is the dipolar field due to the diamagnetic and paramagnetic moments of the molecules in the various capillaries. Let γ_I be the gyromagnetic ratio of the proton. According to the demagnetizing field theory,[28] the dipolar field induces a relative susceptibility shift $\Delta_i\nu(\mathbf{r}_I)/\nu_I$ of the proton resonance frequency $\nu_I = -\gamma_I B_0/(2\pi)$ given by (SI units)

$$\frac{\Delta_i\nu(\mathbf{r}_I)}{\nu_I} = \sum_{j=1}^{n}\left(\frac{1}{3}\delta_{ij} - N_{zz}^{ij}(\mathbf{r}_I)\right)\chi_j \tag{3}$$

where the demagnetizing coefficients $N_{zz}^{ij}(\mathbf{r}_I)$ are defined in terms of integrals over the upper and lower surfaces $S_{\text{up},j}$ and $S_{\text{low},j}$ of the columns C_j of solutions as

$$N_{zz}^{ij}(\mathbf{r}_I) \equiv \frac{1}{4\pi}\int_{S_{\text{up},j}} \frac{(\mathbf{r}_P - \mathbf{r}_I)\cdot\mathbf{k}}{||\mathbf{r}_P - \mathbf{r}_I||^3}\mathrm{d}S_P - \frac{1}{4\pi}\int_{S_{\text{low},j}} \frac{(\mathbf{r}_P - \mathbf{r}_I)\cdot\mathbf{k}}{||\mathbf{r}_P - \mathbf{r}_I||^3}\mathrm{d}S_P \tag{4}$$

The main features of the susceptibility shift are conveniently described in the simplest situation of $n = 2$ molecules and capillaries discussed hereafter. Let u be the symmetry axis of the setup of the two capillaries C_1 and C_2. Denote by π_u the rotation of angle π about u. The demagnetizing coefficients $N_{zz}^{ij}(\mathbf{r}_I)$ are purely geometrical quantities which are invariant under π_u so that we have $N_{zz}^{ij}[\pi_u(\mathbf{r}_I)] = N_{zz}^{ii}(\mathbf{r}_I)$ and $N_{zz}^{ji}[\pi_u(\mathbf{r}_I)] = N_{zz}^{ij}(\mathbf{r}_I)$. The shifts $\Delta_i\nu(\mathbf{r}_I)/\nu_I$ simplify to

$$\begin{aligned}\frac{\Delta_1\nu(\mathbf{r}_I)}{\nu_I} &= \left(\frac{1}{3} - N_{zz}^{11}(\mathbf{r}_I)\right)\chi_1 - N_{zz}^{12}(\mathbf{r}_I)\chi_2 \\ \frac{\Delta_2\nu[\pi_u(\mathbf{r}_I)]}{\nu_I} &= -N_{zz}^{12}(\mathbf{r}_I)\chi_1 + \left(\frac{1}{3} - N_{zz}^{11}(\mathbf{r}_I)\right)\chi_2\end{aligned} \tag{5}$$

and the shift difference becomes

$$\frac{\Delta_2\nu[\pi_u(\mathbf{r}_I)]}{\nu_I} - \frac{\Delta_1\nu(\mathbf{r}_I)}{\nu_I} = \left(\frac{1}{3} - N_{zz}^{11}(\mathbf{r}_I) + N_{zz}^{12}(\mathbf{r}_I)\right)(\chi_2 - \chi_1) \tag{6}$$

In an experimental setup, the height and diameter of the liquid columns typically verify $h \ge 32$ mm and $d \le 1.6$ mm, that is, $h/d \ge 20$, the distance between the axes of the tubes is $\cong 2$ mm, and the length of the detection zone is $l \cong 15$ mm. Then, a straightforward computation shows that the coefficient $(1/3) - N_{zz}^{11}(\mathbf{r}_I) + N_{zz}^{12}(\mathbf{r}_I)$ is equal to the value of 1/3 of the form factor of a tube of infinite height with a precision better than 0.1 %, and eq 6 can be approximated as

$$\frac{\Delta_2\nu[\pi_u(\mathbf{r}_I)]}{\nu_I} - \frac{\Delta_1\nu(\mathbf{r}_I)}{\nu_I} = \frac{1}{3}(\chi_2 - \chi_1) \tag{7}$$

This approximation extends to two points located in C_1 and C_2 at the same height in the NMR tube in the case of two and more capillaries. More generally, if two points $\mathbf{r}_{Ii}$ and $\mathbf{r}_{Ij}$ are located at the same height in two capillaries C_i and C_j amid n parallel capillaries, the difference of the relative frequency shifts at these points is

$$\frac{\Delta_j\nu(\mathbf{r}_{Ij})}{\nu_I} - \frac{\Delta_i\nu(\mathbf{r}_{Ii})}{\nu_I} = \frac{1}{3}(\chi_j - \chi_i) = \frac{1}{3}(\chi_{\text{para},j} - \chi_{\text{para},i}) \tag{8}$$

Note that the possible small curvatures of the upper and lower surfaces $S_{\text{up},j}$ and $S_{\text{low},j}$ due to the menisci and capillary bottoms barely affect eq 8 because these surfaces are at quite large distances $(h - l)/2 \gg d$ from the limits of the detection zone. Furthermore, this equation keeps accurate to within 1 % if the heights of the liquid columns differ by less than about 20 %.

To sum up, the concentrations of paramagnetic solutes dissolved in the different solutions containing the isotopically substituted molecules M_i are chosen according to eq 8 so that the resonance lines of the observed spins are well-separated and do not overlap with the remaining parts of the spectra from the various capillaries.

Susceptibility Frequency Shift Labeling with Ln^{3+} Complexes

We take advantage of the fact that lanthanide Ln^{3+} ions have nearly identical chemistry but magnetic properties which vary

markedly with the number of their 4f inner electrons.[29] First, all paramagnetic Ln^{3+} ions, but not Gd^{3+}, show different, very short electronic relaxation times < 1 ps of their paramagnetic moments,[29,30] so that they weakly accelerate the intermolecular relaxation rates of the surrounding nuclear spins, even at quite large concentrations,[26] $c_{Ln} \cong 100$ mM. In contrast, Gd^{3+} is an ideal paramagnetic ion for magnetic resonance imaging (MRI) contrast agents because of its long longitudinal electronic spin relaxation time[31–34] T_{1e} at the MRI fields[35] ≥ 1 T. Secondly, the heavy paramagnetic Ln^{3+} ions from Tb^{3+} to Yb^{3+} often shift the resonance frequencies of the nuclei of their tightly bound ligands to values outside the chemical shift range of the protons on diamagnetic molecules.[29] Moreover, Gd^{3+} and these heavy Ln^{3+} ions to a lesser extent strongly accelerate the intramolecular relaxation rates and broaden the lines of the nuclei of tightly bound ligands,[29,30] so that these lines tend to disappear in the background noise of the NMR spectrum. Thus, the ligands bound to the Ln^{3+} ions from Gd^{3+} to Yb^{3+} are often NMR silent. Thirdly, the Ln^{3+} ions have significantly different effective magnetic moments $\mu_{eff,Ln}$, for example, $\mu^2_{eff,Gd} = 63$, $\mu^2_{eff,Tb} \cong 94.5$, and $\mu^2_{eff,Yb} \cong 20.6$. The volume paramagnetic susceptibility of an Ln^{3+} complex with magnetic moment $\mu_{eff,Ln}$ and concentration c_{Ln} (mM) is

$$\chi_{para,Ln} = c_{Ln}\mu_0 N_{Avogadro}\frac{\mu^2_{eff,Ln}\mu^2_B}{3k_BT} = 5.27\cdot10^{-9}\frac{298.15}{T}\mu^2_{eff,Ln}c_{Ln} \quad (9)$$

The frequency shifts of the solutions are conveniently obtained by dissolving the two complexes TbL and/or YbL (L = ligand) of short T_{1e} at significant concentrations $c_{Tb} + c_{Yb} \geq 5$ mM and possibly the GdL complex of long T_{1e} at small concentrations $c_{Gd} < 0.5$ mM. The GdL complex acts as an agent for paramagnetic relaxation (rate) enhancement (PRE) and serves to balance the nuclear relaxation rates among the various solutions. In all of the solutions the concentrations of the three complexes are chosen so that their sums keep, as much as possible, a constant value c_{sum}:

$$c_{Tb} + c_{Yb} + c_{Gd} = c_{sum} \quad (10)$$

This requirement ensures that the isotopically substituted molecules M_i move in quasi-identical solutions. In particular, even if the complexes GdL are charged species, the self-diffusion coefficients of ions M_i can be compared directly since these ions undergo the same Coulomb interactions with the complexes. Indeed, the transport properties of a given ionic species often depend significantly on the charges and concentrations of the various ions in the solution.[1,2] Note that we cannot replace YbL by a diamagnetic analogue such as LuL, the proton NMR spectrum of which generally overlaps with the lines of the molecules M_i.

Experimental Section

Purchased Chemicals. Heavy water D_2O (atom fraction $D = 0.999$), methanol CH_3OD (atom fraction $D = 0.99$), methanol CHD_2OD (atom fraction $D = 0.99$), *tert*-butanol $(CH_3)_3COD$ (atom fraction $D = 0.99$), named tBu9OD (9 methyl protons), were purchased from Eurisotop. TPP bromide, the hydrated salts $GdCl_3\cdot6H_2O$, $TbCl_3\cdot6H_2O$, $YbCl_3\cdot6H_2O$, triethylenetetraaminehexaacetic acid H_6ttha, DCl (mass fraction $\omega = 0.35$ in D_2O, atom fraction $D = 0.99$), hypophosphorous acid (mass fraction $\omega = 0.5$ in H_2O), hypophosphorous acid-d_3 (mass fraction $\omega = 0.5$ in D_2O, atom fraction $D = 0.98$), and NaOD (mass fraction $\omega = 0.40$ in D_2O, atom fraction $D = 0.995$) were supplied by Aldrich and used without further purification. Solvents and starting materials for the organic syntheses were purchased from Aldrich, Fluka, or Acros and used without further purification, unless otherwise stated.

Organic Syntheses. ^{1}H NMR spectra were recorded at 25 °C for characterization purposes on a Bruker Advance 200. Chemical shifts are reported in ppm and were referenced internally to the residual solvent resonance. Mass spectra were run on a Thermo Scientific LXQ mass spectrometer equipped with an electrospray source.

tert-Butanol $CD_2H(CD_3)_2COD$. Single hydrogen tBuOD $CD_2H(CD_3)_2COD$, named tBu1OD (1 methyl proton), was prepared as follows. Vaporized iodine crystal was introduced into a flask equipped with stirrer and water-cooled condenser and added to a suspension of Mg (382 mg, 15.9 mmol) in cooled to 0 °C anhydrous Et_2O (10 mL). A Grignard reagent was prepared by adding slowly 2.19 g of methyl-d_2 iodide (CD_2HI, 15.2 mmol) in 15 mL of anhydrous Et_2O (Aldrich). The mixture was stirred at 0 °C for 15 min, heated to reflux for an additional 15 min, and cooled again at 0 °C, and a solution of 1.11 mL of acetone-d_6 (16.7 mmol) in 10 mL of anhydrous Et_2O was added slowly. The cooling bath was removed and the mixture left at room temperature for 30 min. A solution of freshly prepared ND_4Cl (35 mL) was added. The organic and aqueous layers were separated and the aqueous layer extracted 10 times with diethyl ether. The organic layers were combined and dried with Mg_2SO_4, and the major part of diethyl ether was evaporated with caution. The resulting oil was distilled (84 °C) to yield 450 μL of tBuOD (5.6 mmol, 28 % yield), and the purity was confirmed by NMR using two salts as reference [δ_H (200 MHz, D_2O) 1.28 (s, 1H)]. *tert*-Butanol $CH_3(CD_3)_2COD$, named tBu3OD (3 methyl protons) was prepared similarly.

H/D Substituted Tetraphenylphosphonium. The various steps are sketched in Scheme 1.

2,4,6-d_3-Aniline (1). To a 100 mL flask containing 20 g of aniline hydrochloride (0.155 mol) and equipped with a stirrer and a water-cooled condenser 50 mL of D_2O (atom fraction $D = 0.999$) was added. The solution was heated to reflux under nitrogen for 24 h. Water was then removed under reduced pressure and the procedure repeated five times. Sodium hydroxide (1 mol·L^{-1} in water) was then added to the crude dark blue solution, the resulting mixture extracted four times with 200 mL of Et_2O, the organic layers washed with brine and dried with $MgSO_4$, and the solvent removed. **1** was obtained as a colorless oil (7 g, 47 %). ^{1}H NMR (200 MHz, $CDCl_3$): δ = 3.69 (2H, br s, NH_2), 7.19 (2H, s, CH); ES$^+$-MS *m/z*: 97.1 [M + 1]$^+$. The isotopic purity (mass spectroscopy and ^{1}H NMR) was found to be 97 %.

2,6-d_2-4-Bromoaniline (5). Compound **5** was prepared according to the same synthetic procedure described for the synthesis of **1** by using the following: 12.5 g of 4-bromoaniline hydrochloride (0.073 mol), 50 mL of D_2O (atom fraction D = 0.999), and 4 g of DCl (mass fraction $\omega = 0.35$ in D_2O, atom fraction $D = 0.99$). **5** was obtained as a colorless oil (9.53 g, 75 %). ^{1}H NMR (200 MHz, $CDCl_3$): $\delta = 3.79$ (2H, br s, NH_2), 7.29 (2H, s, CH). ES$^+$-MS *m/z*: 174 and 176 [M + 1]$^+$. The isotopic purity (mass spectroscopy) was found to be 98 %.

2,4,6-d_3-Bromobenzene (2). 2,4,6-d_3-Aniline (**1**, 3.64 g, 38 mmol) was dissolved in 48 % aqueous HBr (27 mL). After cooling to 0 °C, sodium nitrite (2.7 g, 39 mmol) was added very slowly to the stirred solution with the temperature being kept within (0 and 5) °C. This diazonium salt solution was then poured into a flask containing CuBr (7.69 g, 53 mmol) and 22

Scheme 1. Synthesis of H/D Substituted Tetraphenylphosphonium Ions

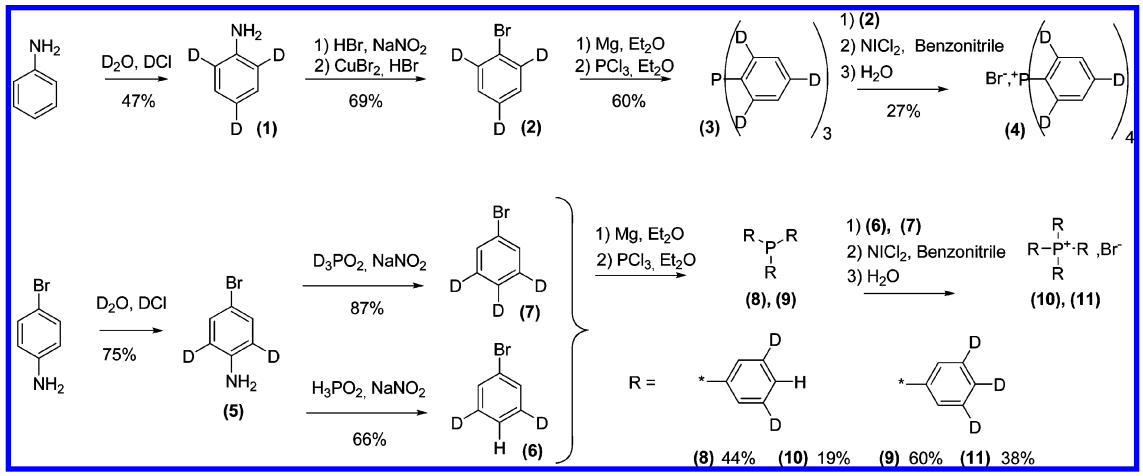

mL of 48 % aqueous HBr. The solution was heated to reflux for 5 h and then extracted three times with dichloromethane. The organic layers were washed with 1 mol·L^{-1} NaOH and water and dried with $MgSO_4$, and the solvent removed. The yellow oil was distillated (51 °C, 27 mbar) to give a colorless liquid (4.2 g, 69 %). ^{1}H NMR (200 MHz, $CDCl_3$): 7.31 (2H, br s, CH).

3,5-d_2-Bromobenzene (6). 2,6-d_2-4-Bromoaniline (**5**, 3.0 g, 17 mmol) was dissolved in 50 % aqueous hypophosphorous acid (3.73 g, 57 mmol) and heated to reflux for 15 min. After cooling to −10 °C, sodium nitrite (573 mg, 8 mmol) was added very slowly into the stirred solution with the temperature being kept within (0 and 5) °C. The stirring was continued at 0 °C for 3 h and then the mixture poured on ice, extracted three times with dichloromethane, and dried with $MgSO_4$. After evaporation of the solvent, the dark oil was distillated (51 °C, 27 mbar) to give a colorless liquid (1.86 g, 66 %). ^{1}H NMR (200 MHz, $CDCl_3$): 7.37 (1H, br s, CH), 7.56 (2H, br s, CH).

3,4,5-d_3-Bromobenzene (7). Compound **7** was prepared according to the same synthetic procedure described for the synthesis of **6** by using the following: 2,6-d_2-4-bromoaniline (**5**, 3.0 g, 17 mmol), 50 % aqueous hypophosphorous acid-d_3 in D_2O (3.90 g, 57 mmol), and sodium nitrite (573 mg, 0.008 mol). After distillation (51 °C, 27 mbar), a colorless liquid was obtained (2.40 g, 87 %). ^{1}H NMR (200 MHz, $CDCl_3$): 7.51 (2H, s, CH).

Tri(2,4,6-d_3-phenyl)phosphine (3). To a 100 mL three-necked flask equipped with a stirrer and a water-cooled condenser entirely flushed with argon to remove the moist air, 592 mg (24 mmol) of fine magnesium turnings and 15 mL of anhydrous Et_2O and iodide were added. A portion of 3.5 g of 2,4,6-d_3-bromobenzene **2** (22 mmol) was then added slowly over a period of 30 min and the mixture heated to reflux for 30 min. After cooling to −10 °C, PCl_3 (1.01 g, 7.4 mmol) was added dropwise to the stirred Grignard solution and the mixture allowed to warm up at room temperature for 30 min. After cooling to 0 °C, water (7 mL) was added, and the resulting mixture was extracted four times with 50 mL of dry Et_2O under argon atmosphere and dried 12 h over Na_2CO_3. After evaporation of the solvent, compound **3** was obtained as a white powder (1.2 g, 60 %) by sublimation (170 °C, 0.5 mbar). ^{1}H NMR (200 MHz, $CDCl_3$): δ = 7.48 (6H, d, J = 2.5 Hz, CH). ES^+-MS: m/z 272.2 $[M + 1]^+$.

Compounds **8** and **9** were prepared according to the same synthetic procedure described for the synthesis of **3** by using the following:

Tri(3,5-d_2-phenyl)phosphine (8). 580 mg (23.9 mmol) of magnesium turnings, 20 mL of anhydrous Et_2O, 3,5-*d*-bromobenzene (**6**, 3.45 g, 21.7 mmol), PCl_3 (993 mg, 7.2 mmol). After sublimation, compound **8** was obtained as a white powder (0.85 g, 44 %). ^{1}H NMR (200 MHz, $CDCl_3$): δ = 7.45 (3H, br s, CH), 7.61 (6H, br s, CH). ES^+-MS m/z: 269.2 $[M + 1]^+$.

Tri(3,4,5-d_3-phenyl)phosphine (9). 334 mg (13.8 mmol) of magnesium turnings, 7 mL of anhydrous Et_2O, 3,4,5-d_3-bromobenzene (**7**, 2.0 g, 12.5 mmol), PCl_3 (572 mg, 4.2 mmol). After sublimation, compound **9** was obtained as a white powder (0.67 g, 60 %). ^{1}H NMR (200 MHz, $CDCl_3$): δ = 7.58 (6H, br s, CH). ES^+-MS m/z: 272.2 $[M + 1]^+$.

Tetra(2,4,6-d_3-phenyl)phosphonium Bromide (4). To a 100 mL three-necked flask equipped with a stirrer and a water-cooled condenser entirely flushed with argon, 1.09 g of compound **3** (4 mmol), 951 mg of anhydrous $NiCl_2$ (4 mmol), 35 mL of anhydrous benzonitrile, and 705 mg of compound **2** (4.4 mmol) were added. The mixture was heated at 190 °C for 24 h. After cooling to 120 °C, water was added (25 mL) and the mixture stirred over a period of 8 h at 120 °C. The yellow mixture was then cooled on ice and filtered and the solid washed with chloroform. The aqueous layer was then extracted four times with chloroform and the organic layers washed with water, dried with $MgSO_4$, and evaporated to dryness to give 750 mg a white-yellow powder. After crystallization in water and drying 2 days under vacuum at 100 °C, compound **4** was obtained as a white powder (470 mg, 27 %). ^{1}H NMR (200 MHz, $CDCl_3$): δ = 7.50 (8H, d, J = 2.9 Hz, CH). ES^+-MS m/z: 351.3 $[M + 1]^+$.

Compounds **10** and **11** were prepared according to the same synthetic procedure described for the synthesis of **4**:

Tetra(3,5-d_2-phenyl)phosphonium Bromide (10). 0.85 g of compound **8** (3.2 mmol), 749 mg of anhydrous $NiCl_2$ (3.2 mmol), 35 mL of anhydrous benzonitrile, and 552 mg of compound **6** (3.5 mmol) were used. After crystallization in water and drying under vacuum, compound **10** was obtained as a white powder (260 mg, 19 %). ^{1}H NMR (200 MHz, $CDCl_3$): δ = 7.43 (4H, br s, CH), 7.68 (8H, br s, CH). ES^+-MS m/z: 347.2 $[M + 1]^+$.

Tetra(3,4,5-d_3-phenyl)phosphonium Bromide (11). 0.65 g of compound **3** (2.4 mmol), 567 mg of anhydrous $NiCl_2$ (2.4 mmol), 25 mL of anhydrous benzonitrile, and 420 mg of compound **7** (2.6 mmol) were used. After crystallization in water and drying under vacuum, compound **11** was obtained as a white powder (390 mg, 38 %). ^{1}H NMR (200 MHz, $CDCl_3$): δ = 7.72 (8H, d, J = 13.4 Hz, CH). ES^+-MS m/z: 351.3 $[M + 1]^+$.

Table 1. Approximate Compositions of the Paramagnetic Solutions Sol1, Sol2, and Sol3 Containing the H/D Substituted Molecules of Methanol, *tert*-Butanol, and Tetraphenylphosphonium in D_2O[a]

solute	Sol1	Sol2	Sol3
methanol (50 mmol·L^{-1})	CH_3OD	no	CHD_2OD
tert-butanol (50 mmol·L^{-1})	tBu9OD	tBu3OD	tBu1OD
TPPBr (20 mmol·L^{-1})	TPP	TP35DP	TP246DP
[Ybttha^{3-}]	7.6 mmol·L^{-1}	3.8 mmol·L^{-1}	0 mmol·L^{-1}
[Tbttha^{3-}]	0 mmol·L^{-1}	4 mmol·L^{-1}	8 mmol·L^{-1}
[Gdttha^{3-}]	0.4 mmol·L^{-1}	0.2 mmol·L^{-1}	0 mmol·L^{-1}

[a] The H/D substituted molecules are for *tert*-butanol $CD_2H(CD_3)_2COD$ (tBu1OD), $CH_3(CD_3)_2COD$ (tBu3OD), and $(CH_3)_3COD$ (tBu9OD) and for tetraphenylphosphonium the fully hydrogenated tetraphenylphosphonium (TPP), tetra(3,5-d_3-phenyl)phosphonium (TP35DP), and tetra(2,4,6-d_3-phenyl)phosphonium (TP246DP). The three solutions contain identical concentrations of the substituted molecules, but different concentrations of the paramagnetic Ybttha^{3-}, Tbttha^{3-}, and Gdttha^{3-} complexes with ttha = triethylenetetraaminehexaacetate leading to different paramagnetic susceptibilities.

Liquid Sample Preparation. Hydrated salts $LnCl_3 \cdot 6H_2O$ were used to prepare the Lnttha^{3-} complexes. Stock solutions of Tbttha^{3-} (99.53 mM), Ybttha^{3-} (100.3 mM), and Gdttha^{3-} (5.0 mM) complexes were prepared by dissolving the appropriate amounts of the hydrated salts $LnCl_3 \cdot 6H_2O$ with H_6ttha in D_2O followed by adjustment of the $pH_{read} \cong 8$ with NaOD solution in D_2O. The precise stoichiometries of the salts were determined by colorimetric titration in acetate buffer (pH 4.5) using standardized H_2Na_2EDTA solution (Merck) and a Xylenol orange indicator. The Lnttha^{3-} stock solution was prepared with a slight relative excess of ligand to avoid the presence of free Ln^{3+} aqua ions. Stock solutions of the various H/D substituted molecules of methanol (500 mM), tBuOD (500 mM), and TPP bromide (35 mM near the solubility limit) were also prepared by dissolving the appropriate amounts of products. The solutions for the diffusion studies with the desired concentrations of H/D substituted molecules and Lnttha^{3-} complexes were obtained by diluting the appropriate volumes of stock solutions with D_2O in 1.5 mL Eppendorf tubes. The Pyrex capillaries (OD = 1.9 mm, ID = 1.5 mm) and the standard NMR tube (5 mm OD precision tube with 0.38 mm wall thickness) serving as a capillary holder were purchased from Wilmad-Labglass.

Diffusion Coefficient Measurement. The self-diffusion coefficients D_X of the various species X in D_2O solutions were measured by a PGSE sequence[20,21] on a 500 MHz Bruker Avance spectrometer equipped with a BBI probe with a triple-axis gradient field. The bipolar stimulated spin−echo sequence was applied to protons on X.[21] Denote the proton gyromagnetic ratio by γ_I, the strength of the gradient pulse by g, the duration of this gradient by δ, and the diffusion delay by Δ. The self-diffusion coefficient D_X of a species X was calculated by fitting of the theoretical expression of the proton signal intensity $I(\delta,\Delta,g) = I_0\exp[-(\gamma_I g\delta)^2(\Delta - \delta/3)D_X]$, where $I(\delta,\Delta,g)$ and I_0 are the intensities in the presence and absence of the gradient pulses, respectively. The values chosen for δ and Δ depend on the magnitude of the measured diffusion coefficient. The values of δ and Δ were typically (4 and 80) ms, respectively. In the experiments g was incremented from (1.18 to 35.4) G·cm^{-1} with a step of 1.18 G·cm^{-1}.

Results and Discussion

As a first illustration of the method, we prepared three solutions Sol1, Sol2, and Sol3 containing the H/D substituted molecules and the Lnttha^{3-} susceptibility shift inducers. The solute concentrations are reported in Table 1 for the three solutions.

The ligand ttha^{6-} was chosen because it completely wraps around the Ln^{3+} ions so that water, and of course methanol, cannot enter the first coordination sphere.[36] In contrast, the popular ligands L for MRI such as dtpa^{5-} (dtpa^{5-} = diethylene triamine pentaacetate) form Ln^{3+} complexes with one coordinating water molecule[37] which can be replaced by methanol.[38] The choice of LnL complexes such as Lnttha^{3-} without coordinating water avoids the formation of LnL−methanol ternary adducts which could slightly modify the self-diffusion coefficient of methanol and somewhat alter the dynamic isotope effects. Because of its limited solubility, we did not use the uncharged complex[39] Lntpatcn (tpatcn = (1,4,7-tris[(6-carboxypyridin-2-yl)methyl]-1,4,7-triazacyclononane) which would not modify the dynamics of the TPP^+ ion by Coulomb interactions.[1,2]

The three solutions were put in three parallel capillaries inside a standard NMR tube as discussed in the Experimental Section. Their ^{1}H 500 MHz spectrum is shown in Figure 2.

All of the lines are well-separated thanks to appropriate susceptibility differences between the solutions. The frequency shift is roughly proportional to the Tbttha^{3-} concentration because this concentration has the most notable variation and Tb^{3+} has the highest effective magnetic moment. Note that the shift variations between Sol2 and Sol1 are somewhat larger than those between Sol3 and Sol2 because the actual Lnttha^{3-} concentrations in Sol2 are about 6 % larger than their target values in Table 1. As predicted by eq 8, the frequency shift variation between two solutions is nearly independent of the observed protons H in all of the molecules but HOD. For instance, the shift variation between Sol3 and Sol2 is $\Delta_{Sol3-Sol1}\nu_{tBuOD}/\nu_H = 0.958$ ppm for the tBuOD protons, but $\Delta_{Sol3-Sol1}\nu_{HOD}/\nu_H = 1.061$ ppm for the HOD protons. The deviation from eq 8 can be explained by significant values of the pseudocontact dipolar interaction H_{pcd} of the HOD proton with the complexed Tb^{3+} ion.[29,38] This interaction stems from the susceptibility anisotropy of Tbttha^{3-} and varies with the distance r_H of the HOD proton to Tb^{3+} as r_H^{-3}. The molecular pair distribution function of the small polar water molecules with respect to the highly charged Tbttha^{3-} ion is expected to be strongly anisotropic[40−43] and to have high peaks for some water/Tbttha^{3-} collision geometries where r_H is small so that H_{pcd} is large. Then, the ensemble average of H_{pcd} over the molecular pair distribution function can also be significant and induce an observable additional relative frequency shift of the water protons. Small values of H_{pcd} can explain the tiny differences of frequency shift variation between two solutions for the observed protons H in all of the molecules but HOD. The concentration c_{Gd} of the PRE agent Gdttha^{3-} is reduced from Sol1 to Sol3 to balance the increase of the nuclear relaxation rates which is due to the Tb^{3+} Curie spin[29,30] and grows with the concentration c_{Tb} of Tbttha^{3-}. Thus, for instance at 25 °C, all of the proton relaxation times are in the range (250 to 800) ms, which is very appropriate for the measurements of the self-diffusion coefficients D_X.

The measured values of D_X are reported in Table 2. Clearly, D_X increases when the molecular mass of the H/D substituted

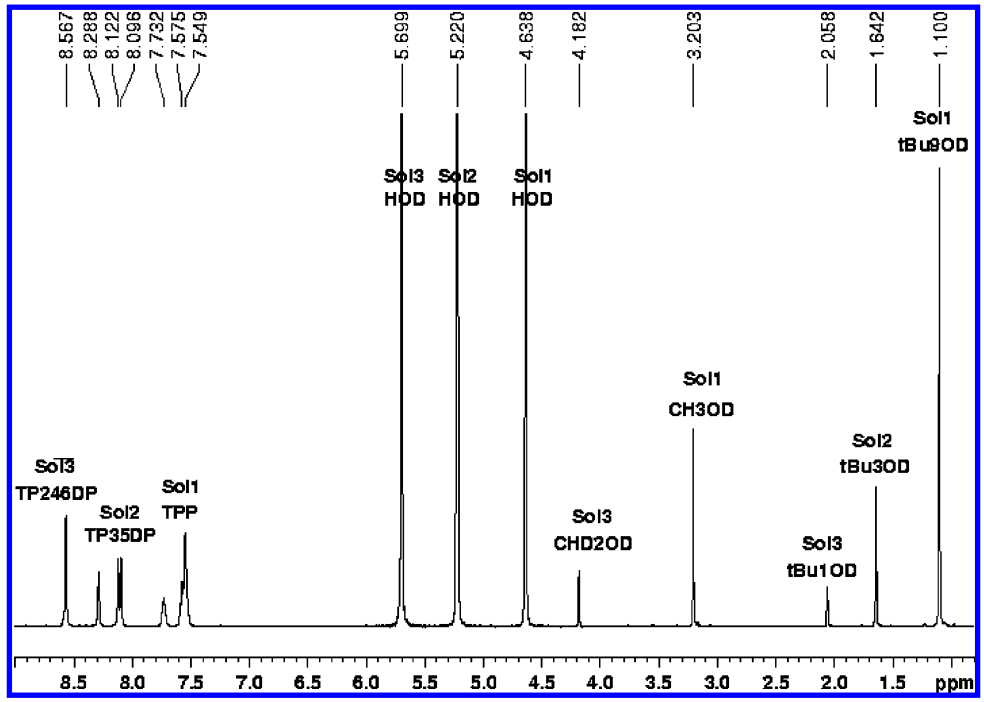

Figure 2. ^{1}H 500 MHz spectrum of the H/D substituted molecules of methanol, tBuOD, and TPP in D_2O at 25 °C. The substituted molecules are dissolved in three solutions Sol1, Sol2, and Sol3 having different paramagnetic susceptibilities and placed in three parallel capillaries inside a standard 5 mm OD NMR tube.

Table 2. Self-Diffusion Coefficients D_X of the H/D Substituted Molecules X in D_2O at the Temperatures (5, 25, and 50) °C

	$D_X/10^{-5}$ cm^2·s^{-1}		
X	t/°C = 5	t/°C = 25	t/°C = 50
TP246DP	0.178	0.360	0.706
TP35DP	0.187	0.366	0.755
TPP	0.187	0.378	0.757
CHD_2OD	0.604	1.13	2.08
CH_3OD	0.639	1.25	2.30
tBu1OD = $CHD_2(CD_3)_2COD$	0.320	0.647	1.30
tBu3OD = $CH_3(CD_3)_2COD$	0.337	0.663	1.39
tBu9OD = $(CH_3)_3COD$	0.336	0.681	1.34

molecule decreases. Typically, the relative increase $\delta D_X/D_X$ is 0.05 for tBuOD or TPP and 0.10 for methanol. The dynamic isotopic effect is smaller for tBuOD or TPP, since the motion of these species, which are significantly larger than the D_2O solvent molecule, should tend toward that of a macroscopic solute for which the Stokes−Einstein expression is valid. Finally, the effect seems to slightly increase with temperature. This work presents preliminary results on self-diffusion. Even with NMR experiments using a restricted number of eight scans, it was possible to detect small variations of the self-diffusion coefficients of rather dilute solutes. The uncertainty on the absolute values of the self-diffusion coefficients D_X measured with the help of the present parallel PGSE experiment is similar to that of the standard experiment with a unique NMR tube and of the order of several percent because of the imprecise calibration of the gradient and RF pulses. This impreciseness does not cause more uncertainty on the differences of the self-diffusion coefficients obtained by the parallel PGSE method and does not affect the accuracy of their ratios under the reasonable assumption that the solutions in the capillaries undergo the same gradient and RF pulses. Then, the uncertainty on these ratios should be intrinsically low and statistically decrease with the number of scans. Note that the spatial homogeneity of the gradient and RF pulses between two capillaries can be checked by repeating the experiments at different rotated positions of the standard NMR tube containing the capillaries. Besides, the use of capillaries should reduce the convection artifacts[21] which become important for nonviscous liquids. We hope that the observation of non-Stokesian self-diffusion effects in simple D_2O by the present method and also in ionic liquids by Wachter et al.[44] will encourage renewed theoretical efforts toward a full understanding of the diffusion process at the molecular level.

Beyond the application to self-diffusion, the aim of this work was to show the experimental potential of the parallel NMR (molecular imaging) method based on solution magnetic-susceptibility differences. In this method, the various liquid solutions are at the same temperature and undergo the same NMR procedure so that the observable quantities can be accurately compared when necessary. More generally, the parallelism of the method leads to a high throughput of data which should facilitate the engineering work. Finally, in the MRI context, it should provide a fast determination of the contrast efficiency of a Gd^{3+} complex GdL, simply by the parallel measurements of the water proton relaxation rates in several GdL solutions with different concentrations of GdL and thus different susceptibilities. Should the susceptibility differences be insufficient, the GdL complexes could be supplemented with the same amount of auxiliary TbL complexes which marginally increase the longitudinal proton relaxation rate.

Acknowledgment

This work is a contribution to the EC COST Action D-38 and European EMIL network. We thank P.-A. Bayle for his help to use the INAC NMR facilities.

Literature Cited

(1) Barthel, J. M. G.; Krienke, H.; Kunz, W. *Physical Chemistry of Electrolyte Solutions*; Springer: Darmstadt, 1998.
(2) Dufreche, J. F.; Bernard, O.; Durand-Vidal, S.; Turq, P. Analytical theories of transport in concentrated electrolyte solutions from the MSA. *J. Phys. Chem. B* **2005**, *109*, 9873–9884.
(3) Hansen, J.-P.; McDonald, I. R. *Theory of Simple Liquids*, 3rd ed.; Academic Press: London, 2006.

(4) Suarez-Iglesias, O.; Medina, I.; Pizarro, C.; Bueno, J. L. On predicting self-diffusion coefficients in fluids. *Fluid Phase Equilib.* **2008**, *269*, 80–92.
(5) Sacco, A.; Belorizky, E.; Jeannin, M.; Gorecki, W.; Fries, P. H. Effective forces between diamagnetic and paramagnetic ions in D_2O at low and moderate ionic strengths: An NMR relaxation study. *J. Phys. II* **1997**, *7*, 1299–1322.
(6) Helm, L. Relaxivity in paramagnetic systems: Theory and mechanisms. *Prog. Nucl. Magn. Reson. Spectrosc.* **2006**, *49*, 45–64.
(7) Kruk, D.; Kowalewski, J. General treatment of paramagnetic relaxation enhancement associated with translational diffusion. *J. Chem. Phys.* **2009**, *130*, 174104.
(8) Bonnet, C. S.; Fries, P. H.; Crouzy, S.; Seneque, O.; Cisnetti, F.; Boturyn, D.; Dumy, P.; Delangle, P. A Gadolinium-Binding Cyclodecapeptide with a Large High-Field Relaxivity Involving Second-Sphere Water. *Chem.—Eur. J.* **2009**, *15*, 7083–7093.
(9) Gierer, A.; Wirtz, K. Molekulare Theorie Der Mikroreibung. *Z. Naturforsch., A: Phys. Sci.* **1953**, *8*, 532–538.
(10) Spernol, A.; Wirtz, K. Zur Mikroreibung in Flussigkeiten. *Z. Naturforsch., A: Phys. Sci.* **1953**, *8*, 522–532.
(11) Edward, J. T. Molecular Volumes and Stokes-Einstein Equation. *J. Chem. Educ.* **1970**, *47*, 261–270.
(12) Mills, R.; Harris, K. R. The Effect of Isotopic Substitution on Diffusion in Liquids. *Chem. Soc. Rev.* **1976**, *5*, 215–231.
(13) Weingartner, H.; Holz, M.; Sacco, A.; Trotta, M. The Effect of Site-Specific Isotopic Substitutions on Transport-Coefficients of Liquid Methanol. *J. Chem. Phys.* **1989**, *91*, 2568–2574.
(14) Holz, M.; Weingartner, H.; Sacco, A. Isotope Effects Upon Translational Diffusion as a Probe for Translation-Rotation Coupling in Molecular Liquids. *Ber. Bunsen-Ges.* **1990**, *94*, 332–336.
(15) Holz, M.; Mao, X. A.; Seiferling, D.; Sacco, A. Experimental study of dynamic isotope effects in molecular liquids: Detection of translation-rotation coupling. *J. Chem. Phys.* **1996**, *104*, 669–679.
(16) Hirschfelder, J. O.; Curtiss, C. F.; Bird, R. B. *Molecular Theory of Gases and Liquids*; Wiley: New York, 1954.
(17) Weingartner, H. Isotopic Effects on the Tracer Diffusion of Water, Methanol and Ethanol Dissolved in Carbon-Tetrachloride at 25-Degrees-C. *J. Chem. Soc., Faraday Trans. 1* **1985**, *81*, 1031–1035.
(18) Wittko, G.; Kohler, W. Influence of isotopic substitution on the diffusion and thermal diffusion coefficient of binary liquids. *Eur. Phys. J. E* **2006**, *21*, 283–291.
(19) Bagno, A.; Rastrelli, F.; Saielli, G. NMR techniques for the investigation of solvation phenomena and non-covalent interactions. *Prog. Nucl. Magn. Reson. Spectrosc.* **2005**, *47*, 41–93.
(20) Callaghan, P. T. *Principles of Nuclear Magnetic Resonance Microscopy*; Oxford University Press: New York, 2003.
(21) Jerschow, A.; Muller, N. Suppression of convection artifacts in stimulated-echo diffusion experiments. Double-stimulated-echo experiments. *J. Magn. Reson.* **1997**, *125*, 372–375.
(22) Evans, D. F. The Determination of the Paramagnetic Susceptibility of Substances in Solution by Nuclear Magnetic Resonance. *J. Chem. Soc.* **1959**, 2003–2005.
(23) Zimmerman, J. R.; Foster, M. R. Standardization of NMR High Resolution Spectra. *J. Phys. Chem.* **1957**, *61*, 282–289.
(24) Loliger, J.; Scheffol, R. Paramagnetic Moment Measurements by NMR - Micro Technique. *J. Chem. Educ.* **1972**, *49*, 646–&.
(25) Piguet, C. Paramagnetic susceptibility by NMR: The "solvent correction" removed for large paramagnetic molecules. *J. Chem. Educ.* **1997**, *74*, 815–816.
(26) Vigouroux, C.; Belorizky, E.; Fries, P. H. NMR approach of the electronic properties of the hydrated trivalent rare earth ions in solution. *Eur. Phys. J. D* **1999**, *5*, 243–255.
(27) Corsi, D. M.; Platas-Iglesias, C.; van Bekkum, H.; Peters, J. A. Determination of paramagnetic lanthanide(III) concentrations from bulk magnetic susceptibility shifts in NMR spectra. *Magn. Reson. Chem.* **2001**, *39*, 723–726.
(28) Belorizky, E.; Fries, P. H.; Gorecki, W.; Jeannin, M. Demagnetizing Field Effects on High-Resolution NMR-Spectra in Solutions with Paramagnetic Impurities. *J. Phys. II* **1991**, *1*, 527–541.
(29) Peters, J. A.; Huskens, J.; Raber, D. J. Lanthanide induced shifts and relaxation rate enhancements. *Prog. Nucl. Magn. Reson. Spectrosc.* **1996**, *28*, 283–350.
(30) Bertini, I.; Luchinat, C.; Parigi, G. *Solution NMR of Paramagnetic Molecules*; Elsevier: Amsterdam, 2001.
(31) Kowalewski, J.; Kruk, D.; Parigi, G. NMR Relaxation in Solution of Paramagnetic Complexes: Recent Theoretical Progresses for $S \geq 1$. *Adv. Inorg. Chem.* **2005**, *57*, 41–104.
(32) Fries, P. H.; Belorizky, E. Electronic relaxation of paramagnetic metal ions and NMR relaxivity in solution: Critical analysis of various approaches and application to a Gd(III)-based contrast agent. *J. Chem. Phys.* **2005**, *123*, 124510.
(33) Fries, P. H.; Belorizky, E. Relaxation theory of the electronic spin of a complexed paramagnetic metal ion in solution beyond the Redfield limit. *J. Chem. Phys.* **2007**, *126*, 204503.
(34) Aman, K.; Westlund, P. O. Direct calculation of ^1H_2O T_1 NMRD profiles and EPR lineshapes for the electron spin quantum numbers $S = 1, 3/2, 2, 5/2, 3, 7/2$, based on the stochastic Liouville equation combined with Brownian dynamics simulation. *Phys. Chem. Chem. Phys.* **2007**, *9*, 691–700.
(35) Caravan, P. Strategies for increasing the sensitivity of gadolinium based MRI contrast agents. *Chem. Soc. Rev.* **2006**, *35*, 512–523.
(36) Chang, C. A.; Brittain, H. G.; Telser, J.; Tweedle, M. F. pH Dependence of Relaxivities and Hydration Numbers of Gadolinium(III) Complexes of Linear Amino Carboxylates. *Inorg. Chem.* **1990**, *29*, 4468–4473.
(37) Caravan, P.; Ellison, J. J.; McMurry, T. J.; Lauffer, R. B. Gadolinium(III) chelates as MRI contrast agents: Structure, dynamics, and applications. *Chem. Rev.* **1999**, *99*, 2293–2352.
(38) Fries, P. H.; Giraud, M.; Belorizky, E. Determination of the rate of a fast exchanging coordinated molecule in a lanthanide(III) complex by proton NMR. *Phys. Chem. Chem. Phys.* **2008**, *10*, 5817–5821.
(39) Fries, P. H.; Gateau, C.; Mazzanti, M. Practical route to relative diffusion coefficients and electronic relaxation rates of paramagnetic metal complexes in solution by model-independent outer-sphere NMRD. Potentiality for MRI contrast agents. *J. Am. Chem. Soc.* **2005**, *127*, 15801–15814.
(40) Fries, P. H.; Kunz, W.; Calmettes, P.; Turq, P. Molecular-Solvent Model for a Cryptate Solution in Acetonitrile - a Hypernetted-Chain Study. *J. Chem. Phys.* **1994**, *101*, 554–577.
(41) Fries, P. H.; Kunz, W.; Calmettes, P.; Turq, P. Small-Angle Neutron-Scattering - a Critical-Study of the Contrast Approximation. *J. Chem. Phys.* **1994**, *101*, 578–584.
(42) Richardi, J.; Fries, P. H.; Krienke, H. The solvation of ions in acetonitrile and acetone: A molecular Ornstein-Zernike study. *J. Chem. Phys.* **1998**, *108*, 4079–4089.
(43) Fischer, R.; Richardi, J.; Fries, P. H.; Krienke, H. The solvation of ions in acetonitrile and acetone. II. Monte Carlo simulations using polarizable solvent models. *J. Chem. Phys.* **2002**, *117*, 8467–8478.
(44) Wachter, P.; Zistler, M.; Schreiner, C.; Fleischmann, M.; Gerhard, D.; Wasserscheid, P.; Barthel, J.; Gores, H. J. Temperature Dependence of the Non-Stokesian Charge Transport in Binary Blends of Ionic Liquids. *J. Chem. Eng. Data* **2009**, *54*, 491–497.

Received for review December 4, 2009. Accepted March 9, 2010.

JE901031B